UC Berkeley
UC Berkeley Previously Published Works

Title
Application of Dislocation Theory to Minimize Defects in Artificial Solids Built with Nanocrystal Building Blocks

Permalink
https://escholarship.org/uc/item/68g6b8tf

Journal
Accounts of Chemical Research, 54(6)

ISSN
0001-4842

Authors
Ondry, Justin C
Alivisatos, A Paul

Publication Date
2021-03-16

DOI
10.1021/acs.accounts.0c00719

Peer reviewed

Application of Dislocation Theory to Minimize Defects in Artificial Solids Built with Nanocrystal Building Blocks

Justin C. Ondry[†,‡] and A. Paul Alivisatos[*,†,‡,¶,§]

†*Department of Chemistry, University of California, Berkeley, California 94720, United States*

‡*Kavli Energy NanoScience Institute, Berkeley, California 94720, United States*

¶*Materials Sciences Division, Lawrence Berkeley National Laboratory, Berkeley, California 94720, United States*

§*Department of Materials Science and Engineering, University of California, Berkeley, California 94720, United States*

E-mail: paul.alivisatos@berkeley.edu

Conspectus

Oriented atomic attachment of colloidal inorganic nanocrystals represents a powerful synthetic method for preparing complex inorganic superstructures. Examples include fusion of nanocrystals into dimer and superlattice structures. If the attachment were perfect throughout, then the resulting materials would have single crystal-like alignment of the individual nanocrystals' atomic lattices. Due to strong electronic coupling of the nanocrystals, this has great promise for realizing materials with emergent phenomena which cannot be achieved with atomic crystals. Unfortunately, experimental realization of these properties has lagged, due to defects that are created during

the attachment. While individual colloidal nanocrystals typically are free of many defects, there are a multitude of pathways which can generate defects upon nanocrystal attachment. These attachment generated defects are typically undesirable, and thus developing strategies to favor defect-free attachment, or heal defective interfaces are essential for the full promise of nanocrystal solids to be realized. There may also be some cases where attachment-derived defects are desirable. In this Account we summarize our current understanding of how these defects arise, in order to offer guidance to those who are designing nanocrystal derived solids.

The small size of inorganic nanocrystals means short diffusion lengths to the surface, which favors the formation of nanocrystal building blocks with pristine atomic structures. Upon attachment, however, there are numerous pathways which can lead to atomic scale defects, and bulk crystal dislocation theory provides an invaluable guide to understanding these phenomena. As an example, an atomic step edge can be incorporated into the interface leading to an extra half-plane of atoms, a one dimensional or line defect known as an edge dislocation. These dislocations can be well described by the Burgers vector description of dislocations, which geometrically identifies planes in which a dislocation can move. Our *in situ* measurements have verified that bulk dislocation theory predictions for 1D defects hold true at few-nanometer length scales in PbTe and CdSe nanocrystal interfaces. Importantly, details of the dislocation geometry greatly influence the kinetics of dislocation removal from the interfaces making some defects easier to heal than others. Ultimately, the applicability of dislocation theory to nanocrystal attachment enables the predictive design of attachment to prevent or facilitate healing of defects upon nanocrystal attachment. We applied similar logic to understand formation of planar (2D) defects such as stacking faults upon nanocrystal attachment. Again concepts from bulk crystal defect crystallography can identify attachment pathways which can prevent or deterministically form planar defects upon nanocrystal attachment. The concepts we discuss work well for identifying favorable attachment geometries for nanocrystal *pairs*, however it is currently unclear how to translate these ideas to near-simultaneous multi-particle attachment, as often may oc-

2

cur in real assembly experiments. Geometric frustration, which prevents nanocrystal rotation, and yet-to-be considered defect generation pathways unique to multi-particle attachment complicate defect free superlattice attachment. New imaging methods now allow for the direct observation of local attachment trajectories, and may enable improved understanding of such multi-particle phenomena. With further refinement, a unified framework for understanding and ultimately eliminating structural defects in fused nanocrystal superstructures may well be achievable in coming years.

Key references

- Ondry, J. C.; Hauwiller, M. R.; Alivisatos, A. P. Dynamics and Removal Pathway of Edge Dislocations in Imperfectly Attached PbTe Nanocrystal Pairs; Towards Design Rules for Oriented Attachment. *ACS Nano* **2018**, *12*, 3178-3189.[1] *In situ TEM studies reveal the importance of dislocation glide plane orientation for facilitating dislocation removal from imperfect interfaces in attached PbTe nanocrystals.*

- Ondry, J. C.; Philbin, J. P.; Lostica, M.; Rabani, E.; Alivisatos, A. P. Resilient Pathways to Atomic Attachment of Quantum Dot Dimers and Artificial Solids from Faceted CdSe Quantum Dot Building Blocks. *ACS Nano* **2019**,*13*, 12322–12344.[2] *Comprehensive in situ TEM studies of dislocation removal pathways in CdSe nanocrystals attached on their prismatic facets.*

1   Introduction

In the macro-world, properties of matter — density, melting point, refractive index — are intensive quantities which are independent of system size. At the nanoscale, this relationship breaks down and many materials' properties become strongly system-size dependent. Inorganic colloidal nanocrystals simultaneously display strongly size dependent thermodynamic (*e.g.* melting point[3] and phase transitions[4]) and electronic properties.[5] As such, under-

standing the size dependent thermodynamic and kinetic properties related to growth are crucial to engineering size dependent electronic structures. Electronic structure engineering using handles such as size, shape, doping, and composition variation, can be used to tailor make structures for various applications (*e.g.* efficient light emission, charge separation, etc). As isolated nanocrystals, high-quality samples are routinely achieved. However for many practical applications nanocrystals must be brought close enough for electronic communication. Atomic attachment of individual nanocrystals enables strong electronic communication between nanocrystals, however challenges need to be overcome to realize high-quality nanocrystal attachment.

In this Account we will discuss thermodynamic and kinetic factors which dominate at the nanoscale and favor the formation of defect-free inorganic nanocrystals. Next we will discuss atomically attaching individual nanocrystals into crystallographically fused superstructures. We will focus on attachment mediated defect formation and removal pathways. Our recent *in situ* TEM experiments document defect removal pathways in imperfectly attached PbTe[1] and CdSe[2] pairs and point towards the possibility of a unifying framework to understand and control defects in attached inorganic nanocrystals. Finally we will discuss progress and challenges of translating nanocrystal pair attachment principles to attachment of nanocrystal arrays.

1.1   Imperfections in (nano)crystalline solids

The small size of colloidal nanocrystals changes kinetic considerations taken for granted in bulk materials. In a bulk crystal (Figure 1A) there are typically imperfections with high energy configurations throughout the volume. Long diffusion distances to surfaces, where these defects can be expelled, make their removal slow and difficult. In contrast, in colloidal nanocrystals (Figure 1B) a free surface is at most a few nanometers away and high energy imperfections can easily be expelled to the surface. In Figure 1C we consider the size scaling of the time required for a vacancy to diffuse to the surface of CdS crystallites, highlighting

the benefit of small crystallites. As a result only defects whose energy are sufficiently low to be present at thermodynamic equilibrium are present (Figure 1B).
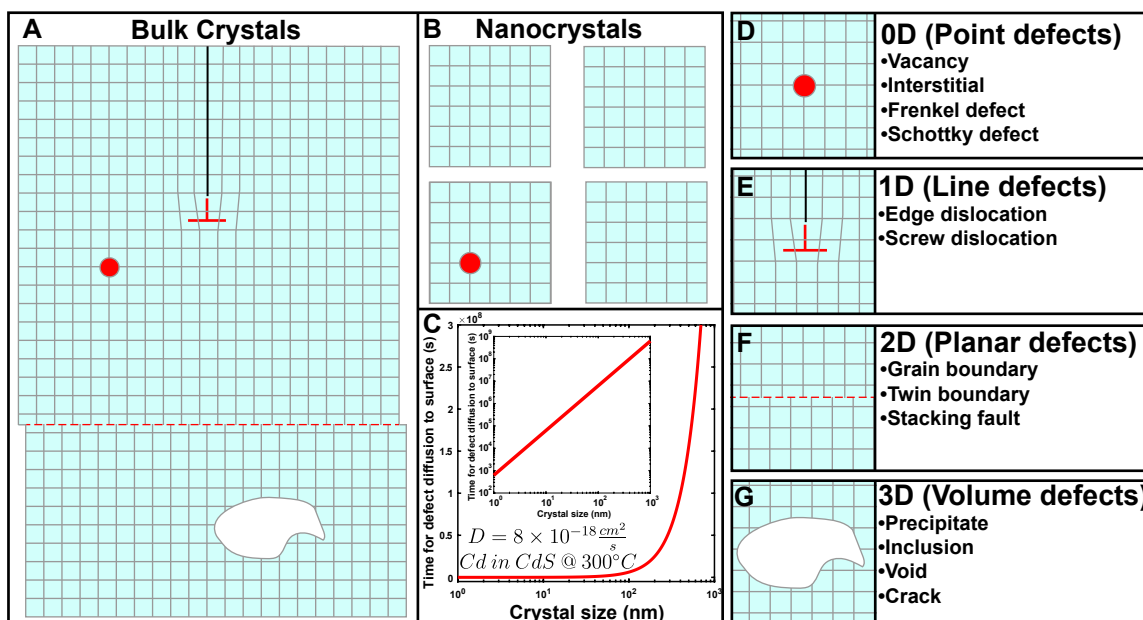

Figure 1: Crystals and imperfections. (A) A bulk crystal schematic with different structural defect classes, and (B) nano-sized crystals which are typically devoid of non-equilibrium structural defects. (C) Plot of the average time it takes to expel a vacancy in CdS crystallite as a function of crystallite size at 300˚C. The the vacancy diffusion coefficient was calculated from Woodbury.[6] (D-G) Classification of structural defects with increasing dimensionality.

To better understand imperfections in crystalline solids, we consider the different classes explicitly. We begin with 0D point defects (Figure 1D), such as vacancies. Vacancies are often considered *equilibrium* defects, since their formation energies are small enough that that they exist at equilibrium at finite temperatures. The addition of an extra half-plane of atoms leads to an edge dislocation which represents a class of 1D defects (Figure 1E). For a 1D defect spanning a crystal, the energy scales with the length and can approach $5\frac{eV}{\text{Å}}$, automatically making them non-equilibrium defects.[7] Termination of a lattice plane within a crystal leads to atoms which have dangling bonds, and thus typically represent trap states in semiconductors.[8] For 2D planar defects such as grain boundaries (Figure 1F) the energy scales with area, again resulting in large formation energies. Special cases of 2D defects, such as twin boundaries and stacking faults, can have quite low formation energies.[9]

Similar, unfavorably high formation energies are present for 3D volume defects (Figure 1G). Typically, 0D defects (Figure 1E) have appreciable thermodynamic concentrations at finite temperatures ($k_b T$) and all other classes are considered non-equilibrium defects since they are (typically) kinetically trapped. On these grounds alone, one could anticipate that, based on the facile kinetics of 0D defect removal, it ought to be possible to prepare exceptionally high-quality initial nanocrystal building blocks. On thermodynamic grounds the high energies of 1D and 2D defects suggest that with the right pathway, it might be possible to attach these building blocks into pristine nanocrystal solids. How to think about such pathways is the subject of this Account.

The short diffusion lengths in nanocrystals facilitate removal of non-equilibrium defects. As a result, structurally pristine colloidal nanocrystals can be synthesized at low temperatures compared to bulk melting temperatures. An example of a single crystal wurtzite CdSe nanocrystal is shown in Figure 2A which appears free of structural imperfections (except at stacking fault at the bottom). Through appropriate heterostructure fabrication and surface passivation, CdSe/CdS core shell semiconductor nanocrystals with luminescence efficiency (quantum yield 99.6±0.2%), which is a proxy for crystal quality, have recently been achieved (Figure 2B).[10] This quantum yield is comparable to MBE and MOCVD grown semiconductor heterostructures. As such, individual colloidal semiconductor nanocrystals are tantalizing building blocks for complex, semiconductor assemblies and superlattices.

1.2 Opportunities and challenges in nanocrystal attachment

Atomically fused nanocrystals present exciting opportunities because the all-inorganic interface allows for strong electronic coupling (Figure 2C).[11] Subsequently, this can lead to electronic mini-bands which can be engineered in ways atomic bands cannot.[12] However, synthetic pathways for translating individual nanocrystals to pristine attached particles remains unclear. An example of an atomically fused nanocrystal dimer of CdSe/CdS is shown in Figure 2D.[13] Expanding attachment to multiple particles results in, for example, honey-

comb lattices of atomically fused PbSe nanocrystals (Figure 2E).[14] Unfortunately many of the predicted properties (such as Dirac mini-bands[12] and non-trivial flat bands[12]) of these materials remain elusive, likely due to imperfections in the materials.[15]
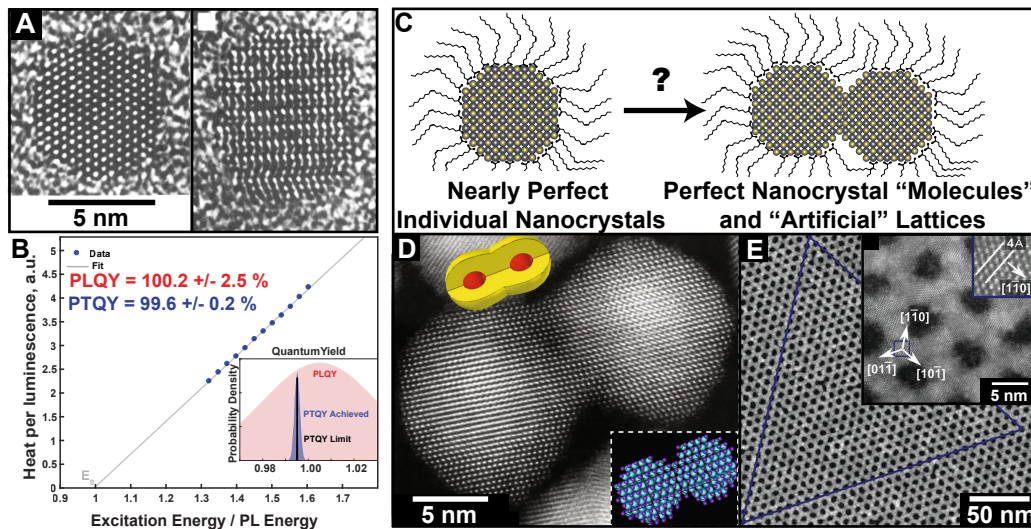

Figure 2: From high-quality individual nanocrystals to attached superstructures. (A) Example of a single crystal wurtzite CdSe nanocrystal. Reproduced with permission from ref 16. Copyright 1995 American Chemical Society. (B) Near-unity quantum yield CdSe/CdS quantum dots. Reproduced with permission from ref 10. Copyright 2019 AAAS. (C) Scheme outlining the challenges converting individual nanocrystals into atomically fused superstructures. (D) Example of an atomically fused CdSe/CdS quantum dot dimer. Reproduced with permission from ref 13. Copyright 2019 Nature Publishing Group. (E) Example honeycomb lattice derived from individual PbSe nanocrystals. Reproduced with permission from ref 14. Copyright 2014 AAAS.

In this Account, we will consider defect generation upon atomic attachment of individual nanocrystals. We will highlight how our recent *in situ* TEM studies of imperfect nanocrystal attachment which point to design principles for enhancing defect removal prospects or preventing their formation.[1,2] In Section 2, we will discuss sources of imperfections resulting from nanocrystal attachment. In Section 3, we will present a dislocation theory framework for rationally describing 1D dislocations in imperfect interfaces. Next in Section 4, we will consider 2D planar defects such as stacking faults and present design principles to control or prevent their formation. Finally in Section 5 we will consider multiple-nanocrystal attachment and the additional complications which result. We will highlight progress in

improving attachment quality and opportunities for additional study regarding atomically fused nanocrystal superlattices. Together we hope this Account provides a road map for mitigating structural imperfections in attached colloidal nanocrystals much like well-established strategies in traditional crystal growth.

2 Defect generation from nanocrystal attachment

We begin by considering possible configurations for nanocrystal attachment in otherwise pristine nanocrystals. Broadly, to achieve atomic attachment of colloidal nanocrystals, the particles must be oriented with a common crystal alignment. This is typically achieved by rotation of nanocrystals in solution,[17] or via shape engineering.[18] First, in Figure 3A, two crystals with atomically flat surfaces can seamlessly join. Experimental examples such as Figure 3E reveal pristine attachment is indeed possible.

Next in Figure 3B we consider the attachment of two nanocrystals, one which contains an atomic step on the faceted surface. In this case, the atomic step is incorporated into the interface, leading to the formation of an edge dislocation (1D defect) trapped at the interface. Figure 3F-H all show examples of edge dislocations in TiO_2, PbSe, and iron oxyhydroxide respectively. Alternatively edge dislocations could result from nanocrystals held at a misttilted angle (Figure 3, and upon attachment, diffusion into the interface incorporates an extra half-plane of atoms.

Another possibility is shown in Figure 3D where two atomically smooth nanocrystals can attach with a fractional unit cell translation, leading to a metastable stacking fault at the interface. Figure 3I shows an example of a stacking fault in attached $CsPbBr_3$ nanocrystals. Analogously, nanocrystals can attach resulting in a twin boundary (Figure 3J). Taken together, Figure 4A-D represent several major pathways which can lead to imperfections upon pristine particle attachment.
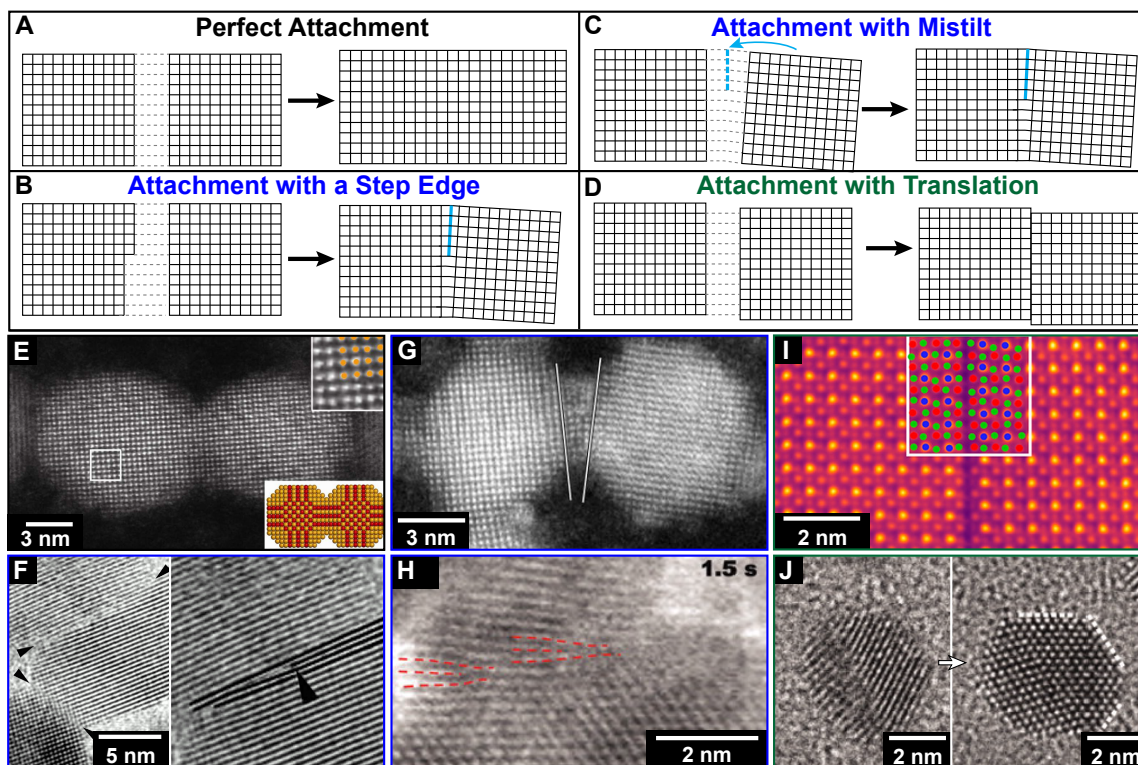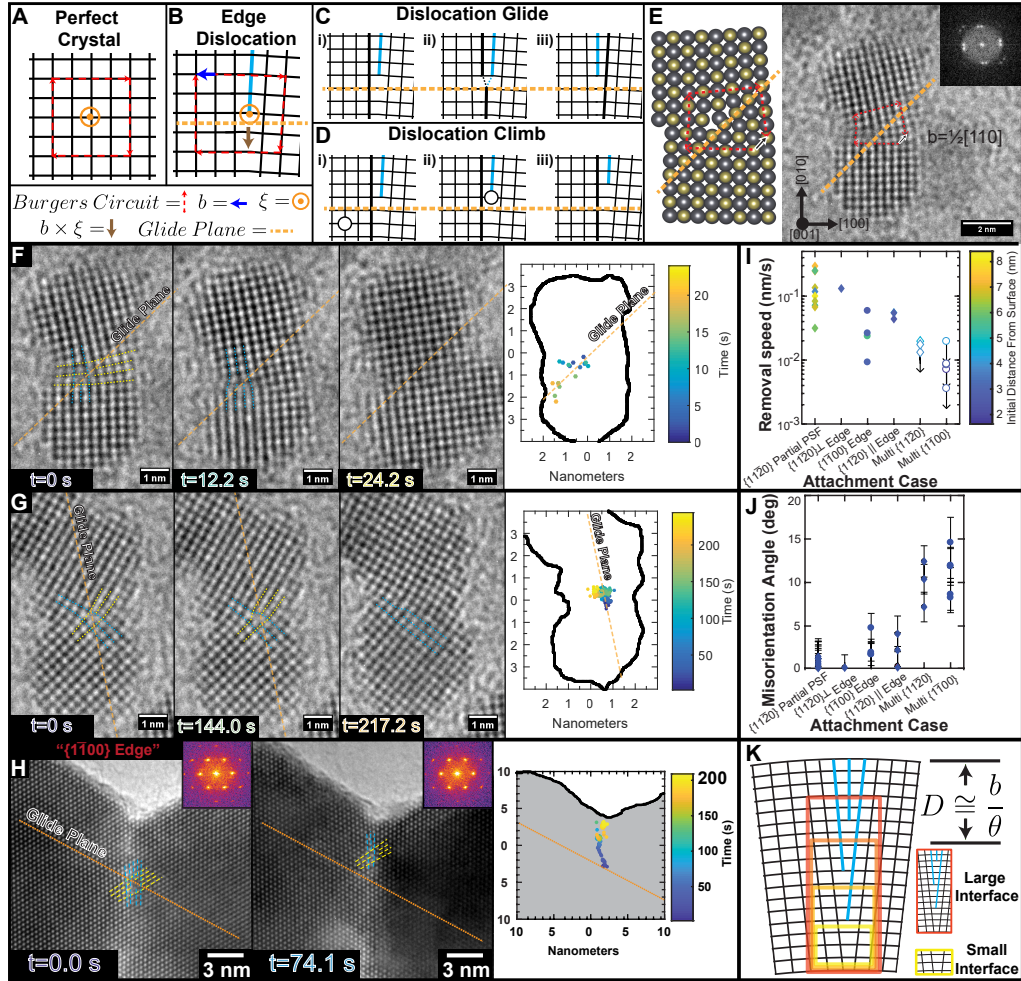
Figure 3: Defect generation pathways during nanocrystal attachment. (A) Perfect attachment, (B) Attachment of particles with a step edge , (C) Attachment with a mistilt, and atomic diffusion into the interface, and (D) attachment with a translation leading to a stacking fault. (E) Example of perfect attachment of PbSe nanocrystals. Reproduced with permission from ref 19. Copyright 2013 American Chemical Society. (F-H) Examples of edge dislocations resulting from nanocrystal attachment in TiO_2, PbSe, and iron oxyhydroxide nanocrystals respectively. (F) Reproduced with permission from ref 20. Copyright 1998 AAAS. (G) Reproduced with permission from the supporting information of ref 19. Copyright 2013 American Chemical Society. (H) Reproduced with permission from ref 17. Copyright 2012 AAAS. Example of stacking fault (I) and twin (J) planar defects resulting from nanocrystal attachment in $CsPbBr_3$ and Pt respectively. (I) Reproduced with permission from ref 21. Copyright 2018 American Chemical Society. (J) Reproduced with permission from ref 22. Copyright 2012 AAAS.

3   Edge dislocations

Edge dislocations often result from particle attachment and warrant careful study.[20] We first consider formal definitions of dislocation geometry which can dictate the directions a defect can move within a crystal. In the case of a perfect crystal, any closed circuit of translations spanning the same number of atoms returns to the original starting point (Figure 4A). This is known as a Burgers circuit (red dashed line).[23] In the case of an inserted half-plane (light blue), a similar circuit does not return to the starting position (Figure 4B). Instead, the vector needed to close the circuit (dark blue arrow) is defined as the Burgers vector. The line running along the dislocation core is defined as the sense vector, ξ, (orange vector perpendicular to the page). Edge dislocations result when b and ξ are orthogonal and screw dislocations are the case where b and ξ are co-linear.[7] The plane defined by the cross product of the Burgers vector and sense vector, $b \times \xi$, (brown arrow) is the glide plane (orange dashed line), and is where a dislocation can move the easiest.[7]

To understand why a dislocation can move easily in it's glide plane we consider Figure 4C where the extra half plane of atoms can move in the lattice via simple atomic rearrangements at the terminus of the half-plane. Gliding of a dislocation is conservative (*i.e.* doesn't require addition or removal of atoms) and is only possible within the glide plane.[7] For movements in directions out of the glide plane, a net flux of atoms is needed. For example in Figure 4D, coalescence of a vacancy with the half-plane leads to movement perpendicular to the glide plane ("climb"). Typically dislocation climb is slower than glide since vacancies have a limited concentration.[23]

An example of Burgers vector and glide plane determination in a model and experimental HRTEM image of PbTe nanocrystals imperfectly attached on {100} facets are shown in Figure 4E. Section S1 gives a review of miller index system. In this case we observe a $b = \frac{a}{2}\langle 110 \rangle$ edge dislocation indicating the magnitude "$\frac{a}{2}$" and direction "$\langle 110 \rangle$" of the Burgers vector. In this case, the glide plane for the dislocation intersects the surface of the attached particles, providing a pathway to the surface. We used *in situ* high resolution

Figure 4: Rational description of edge dislocations in attached nanocrystals. Burgers circuit for a (A) perfect crystal and an (B) edge dislocation. The plane defined by "$b \times \xi$" is the glide plane (orange dashed line). (C) Mechanism for dislocation glide and (D) climb. (E) Example Burgers circuit for a model (left) and experimental HRTEM image (right) for an imperfect interface in rock salt PbTe with a $b = \frac{a}{2}\langle 110 \rangle$ edge dislocation. (F) Example *in situ* HRTEM trajectory of imperfectly {100} attached PbTe nanocrystals with a $b = \frac{a}{2}\langle 110 \rangle$ dislocation. (G) Example trajectory of imperfectly {110} attached PbTe nanocrystals with a $b = \frac{a}{2}\langle 110 \rangle$ dislocation. (E-G) Reproduced from ref 1. Copyright 2018 American Chemical Society. (H) Example trajectory of imperfectly {1$\bar{1}$00} attached of wurtzite CdSe nanocrystals with a $b = \frac{a}{3}\langle 11\bar{2}0 \rangle$ edge dislocation. (I) Classification of dislocation removal speeds and (J) atomic lattice misalignment in imperfectly attached CdSe. (K) Analytic model to predict the number of dislocations for misoriented nanocrystals of a given size. (H-K) Reproduced with permission from ref 2. Copyright 2019 American Chemical Society.

11

TEM at controlled electron beam dose rates to simulate thermal annealing and to track the dislocation position (Figure 4F) throughout the trajectory. Indeed the dislocation follows the glide plane to the surface, resulting in a defect free interface after ∼24s.

We next considered attachment on {110} facets (Figure 4G). We observe the identical dislocation type ($b = \frac{a}{2}\langle 110 \rangle$), but it's glide plane is co-linear with the attachment direction, resulting in a geometry with no direct glide pathways to the surface. During a total observation time of ∼250s, the defect does not leave the interface. Based on our results, glide plane orientation relative to the surface dictate dislocation removal kinetics in attached PbTe nanocrystals. This concept may be a powerful tool for identifying attachment facets which may facilitate defect removal, should one form.

Subsequently we studied wurtzite CdSe nanocrystal attachment on prismatic facets. For wurtzite we use the Miller-Bravais indexing system (Section S1). We observed different classes of defects including edge dislocations, stacking faults, and partial dislocations, due to the complex dislocation landscape in wurtzite.[24,25] Imperfect attachment on {1$\bar{1}$00} facets (Figure 4H) results in an edge dislocation with $b = \frac{a}{3}\langle 11\bar{2}0 \rangle$ Burgers vector. The dislocation glide plane does not provide a pathway to the surface. Interestingly, the interface is successfully healed under simulated annealing in a TEM *via* dislocation climb. Currently it is unclear why dislocations climb in attached CdSe, but not in the PbTe. These results demonstrate activating dislocation climb enables additional dislocation geometries be expelled from an imperfect interface.

Several dislocation types were identified in attached CdSe nanocrystals. Through extensive *in situ* TEM experimentation, we identified the relative ease of removal for each defect type (Figure 4I). While the details of these trends is nuanced, overall a larger mistilt of the atomic lattice (Figure 4J) leads to slower defect removal. This suggests minimizing the angle between particles results in defect which can be more easily removed. This can be understood by considering imperfect nano-interfaces as snapshots of a low angle tilt boundary (Figure 4K) where the dislocation spacing, D is approximated by $D \sim \frac{b}{\theta}$. For larger

12

interfaces or larger tilt angles, *two* dislocations are more likely to be incorporated. Multiple dislocations can (attractively) interact *via* their strain field,[7] hampering removal. In practice, parameters to control relative particle orientation before attachment are unclear. In cases where step edges lead to defects (Figure 3B), developing synthetic methods for step-edge free nanocrystals are needed. Atomic step energies on crystals can vary from $0.01\frac{eV}{\text{Å}}$ to $1\frac{eV}{\text{Å}}$ indicating surface steps on nanocrystals may have a *thermodynamic* concentration.[26] In cases where forced mistilt from geometric frustration lead to dislocation formation (Figure 3C), self assembly strategies leading to uniform atomic alignment are needed.

3.1 Dislocation nano-mechanics

Many phenomena of dislocations in bulk materials can be understood using continuum elasticity methods.[7] A defective nanocrystal interface represents a test case for ultra small scale defect behaviors. First, we consider the forces acting on a dislocation at a free surface using the image dislocation model (Figure 5A).[7] Continuum elasticity predicts an attractive force the closer the dislocation is to the surface. This would result in defects initially closer to a free surface displaying higher average speed ($\frac{distance}{time}$) for removal. Indeed Figure 5B qualitatively shows this trend for dislocations in PbTe nanocrystals. Finally, strong surface-attractive forces, which *drive* dislocations out of small crystallites, are a manifestation of contentious "self-purification"[27–29] in colloidal nanocrystals.

Next we consider the mistilt between two particles with a single dislocation at the interface (Figure 5C). The angle (β) between the particles is determined by the interface thickness (t), Burgers vector (b), and dislocation position(y) and has been explored for large crystals.[30] At the nanoscale, it predicts that a dislocation leads large mistilt and successfully predicts the mistilt between PbTe nanocrystals (Figure 5D). Imperfect attachment provides a useful test-bed for single nanometer nano-mechanics. At these length scales well known phenomena are much more dramatic than in larger systems. Future experiments will further our understanding of the mechanical properties of inorganic nanocrystals.
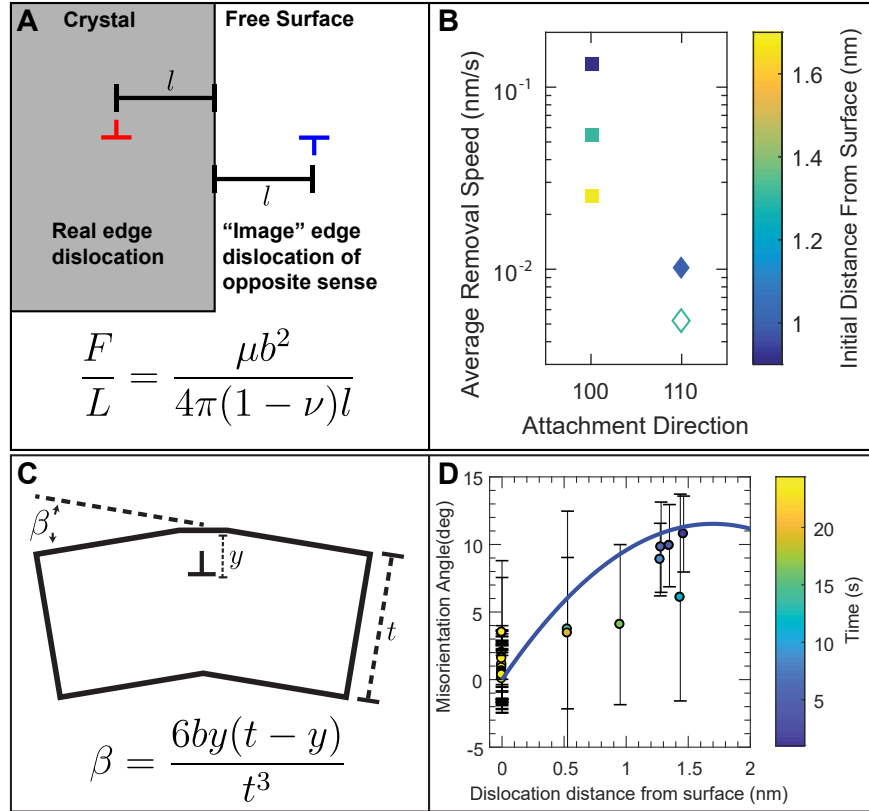
Figure 5: Nanocrystal attachment as a test-bed for nanoscale mechanics. (A) Forces on a dislocation at a free surface where $\frac{F}{L}$ is the force per unit length on the dislocation, μ is the shear modulus, b is the Burgers vector, ν is Poisson's ratio, and l is the distance from the surface. (B) Increased removal speed for dislocations which are initially closer to the surface. (C) Continuum mechanics prediction for dislocation induced mistilt, β, as a function of interface thickness, t, dislocation position, y, and Burgers vector, b. (D) Experimental mistilt between two PbTe nanocrystals as a function of dislocation position with the analytical result of the equation in (C) plotted in blue. Reproduced with permission from ref 1. Copyright 2018 American Chemical Society.

4 Planar defects

Unlike dislocations, which have a disrupted local bonding environment at the core of the dislocation, certain planar defects have minimal disruption to the local bonding environment. Thus certain planar defects are only slightly higher in energy compared to a pristine structure and can be stable minima in the potential energy landscape. We aim to develop design principles to controllably form (or avoid) planar defects resulting from nanocrystal attachment. To illustrate a conceptual framework for identifying attachment geometries which can control planar defect formation, we consider translating part of a honeycomb lattice (Figure 6A) along "zig-zag" and "armchair" planes (blue and green respectively). In "zig-zag" translations, alternative bonding geometries are not possible, and no meta-stable energetic minima result. Alternatively "armchair" translations of $\frac{1}{2}$ unit cell, result in a 4-8 membered ring geometry which is a metastable bonding configuration. This example illustrates the importance of facet geometry in designing defect free interfaces.

Now we consider the case of wurtzite CdSe nanocrystals on their prismatic ($\{1\bar{1}00\}$ and $\{11\bar{2}0\}$) facets. In wurtzite, a $\{11\bar{2}0\}$ prismatic stacking fault is possible and results in a metastable 4-8 membered ring.[36] In the case of attachment on $\{1\bar{1}00\}$ ("zig-zag") facets (Figure 6B), the planes which can have a prismatic stacking fault (green) do not coincide with an attachment facet, and as such only the attachment geometry in Figure 6C is observed. In the case of $\{11\bar{2}0\}$ ("armchair") attachment, the attachment plane coincides with a plane which can have a prismatic stacking fault . Thus two possibilities exist: perfect attachment (Figure 6D) or a half unit cell translation leading to a prismatic stacking fault (Figure 6F). Experimentally both perfect (Figure 6E) and prismatic stacking fault (Figure 6G) interfaces are observed for $\{11\bar{2}0\}$ facets. This comparative example illustrates how attachment facet can dictate which planar defects form.

Some planar defects represent metastable structures, and thus resist returning to the perfect lattice structure. We observed that a prismatic stacking fault persisted over 300s of simulated annealing (Figure 6H).[2] This demonstrates the importance planar defects resulting
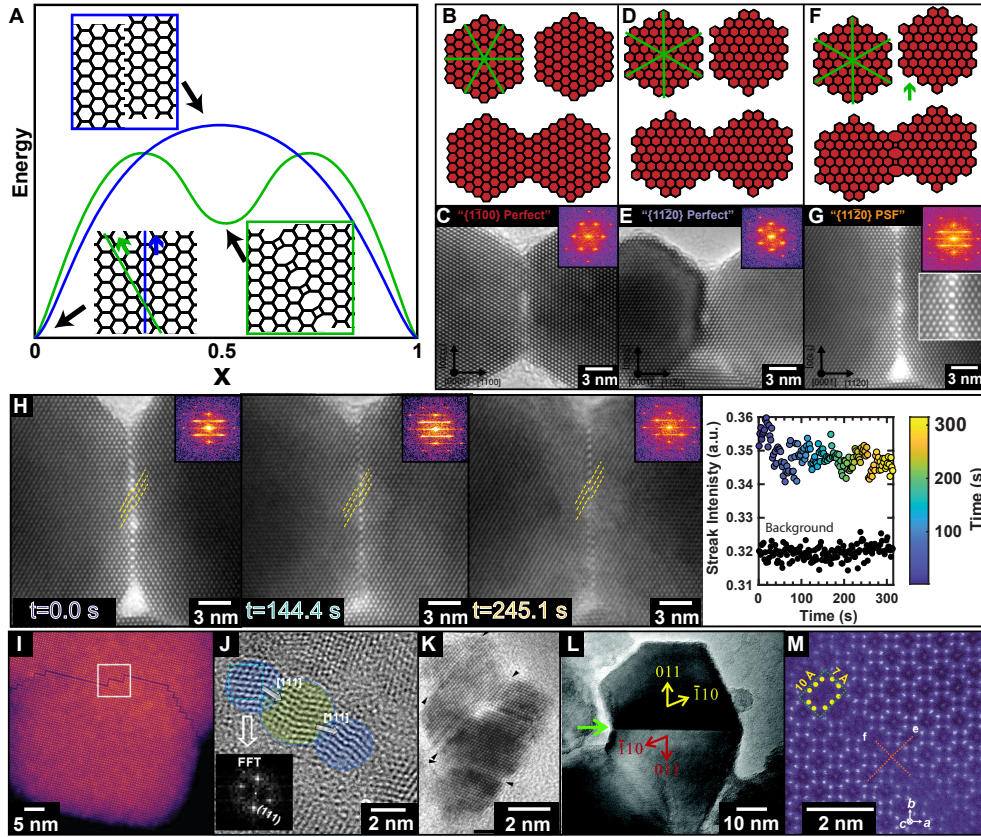
Figure 6: A framework for determining planar defect formation. (A) Relative energy for translating a honeycomb crystal along "zig-zag" (blue) and "armchair" planes (green). (B,C) Attachment of wurtzite CdSe on $\{1\bar{1}00\}$ (zig-zag) facets allows only perfect attachment. Planes where prismatic stacking faults can form are highlighted in green. (D-G) Attachment of wurtzite CdSe on $\{11\bar{2}0\}$ (armchair) facets has two possibles. (D,E) Perfect attachment, (F,G) and formation of a prismatic stacking fault. (H) *in situ* HRTEM showing the stability of a prismatic stacking fault during simulated annealing. (C,E,G,H) Reproduced with permission from ref 2. Copyright 2019 American Chemical Society. (I) Example of Ruddlesden Popper defect in perovskite $CsPbBr_3$ nanocrystals attached on $\{100\}$ facets. Reproduced with permission from ref 31. Copyright 2018 American Chemical Society. (J) Basal plane stacking faults and twins in wurtzite/zinc blende ZnS nanocrystals attached on $\{0001\}$ facets. Reproduced with permission from ref 32. Copyright 2013 American Chemical Society. (K) Multiple planar defects in attached ZnS. Reproduced with permission from ref 33. Copyright 2003 American Chemical Society. (L) Twin boundary resulting from attachment of TiO_2 nanocrystals on $\{011\}$ facets. Reproduced with permission from ref 34. Copyright 2004 American Chemical Society. (M) 2×3 tunnel defects in α-MnO_2. Reproduced with permission from ref 35. Copyright 2016 American Chemical Society.

from attachment since they are difficult to remove. Alternatively this presents an exciting opportunity for planar defect engineering. Some planar defects may harbor useful electronic structures,[37] and imperfect (but intentional) attachment may provide a route to high density and possibly even periodic arrangements of such useful imperfections.

Examples of this are already present in the literature. For example in $CsPbBr_3$, and other perovskite crystal structures Ruddlesden-Popper defects which lie in {100} planes are well known imperfections.[38] Coincidentally, colloidal nanocrystals of $CsPbBr_3$ are usually terminated with {100} facets. Atomic attachment of $CsPbBr_3$ nanocrystals results in Ruddlesden-Popper defects, one such example is shown in Figure 6I. Similarly in the case of attaching wurtzite/zinc blende materials on {0001}/{111} facets, twin boundaries, stacking faults, and coherent phase boundaries can all lie in that plane. Such variety of defects are readily observed in for example {0001} attached ZnS nanocrystals (Figure 6J) and in hydrothermally coarsened ZnS (Figure 6K). Additional examples of controlled planar defect formation in TiO_2 and α-MnO_2 are also shown in Figure 6L and M. Ultimately facet specific attachment of colloidal nanocrystals may enable deterministic fabrication of metastable planar defects which are in and of themselves useful.

5   Considerations for multiple particle attachment

Thus far we have focused on cases of 2-particle attachment and shown principles from traditional dislocation theory which explain experimental results in PbTe and CdSe. One of the goals alluded to in Figure 2E is to prepare semiconductor superlattices via attachment of many nanocrystals. For multiple particle attachment there are additional complications. For example it has been show that attachment of a 3rd particle across two already mistilted particles results in the formation of a screw dislocation (Figure 7A).[20] Another possible formation mechanism, which does not need to invoke a step edge is shown in Figure 7Bi where one nanocrystal differs in size by a single atomic layer (bottom right). Upon attachment, an

17

extra half-plane is incorporated in the upper interface. This would result in an aptly named "hollow-core" edge dislocation.[39] In Figure 7Bii, we show an atomic resolution STEM image of attached PbSe nanocrystals collected by Savitzky *et al.*.[40] We overlaid Burgers circuits of a perfect 4 crystal junction (orange) and a hollow core dislocation (red). See Figure S 3 and Figure S 4 for additional examples in PbSe and CdSe respectively. The additional complications related to multi-particle attachment create further hurdles in realizing high-quality nanocrystal arrays.

In considering the expansion of few-particle attachment to array attachment, the complexity increases rapidly, and explicitly considering individual attachment events is difficult. In an ideal single crystal, the atomic lattice has one orientation present. Angular mistilts, as we have seen, lead to dislocations and can provide a useful proxy for estimating dislocation density.[44] Local atomic lattice orientation measurements by Dasilva *et al.* using 4D STEM of attached PbSe nanocrystals have enabled identification of the 3D atomic lattice orientation (Figure 7C iii and iv). These measurements coupled with measurements of superlattice order parameters (ψ_4) (Figure 7C i and ii) provide a detailed understanding of the coupled atomic and mesoscale order. The ultimate goal is to identify the assembly/attachment conditions and post-processing, leading to each nanocrystal achieving the same atomic lattice orientation. Towards that goal, Smeaton *et al.* performed *in situ* annealing on a superlattice of attached PbSe nanocrystals (Figure 7D).[42] Measurement of the out of plane tilt of individual nanocrystals shows that thermal annealing increases the uniformity in a small field of view. To probe the improved atomic alignment on larger length scales Walravens *et al.* used $2\theta - \Omega$ XRD scans to highlight improved atomic alignment across large area films upon thermal annealing. (Figure 7E)[43]

Careful atomic lattice orientation mapping presented in Figure 7C highlights the considerable variability in attached semiconductor superlattices, and the implicit lower crystal quality due to tilt induced dislocations and strain. As such, developing strategies for improving alignment of particles during assembly, attachment, or post-synthetically represent
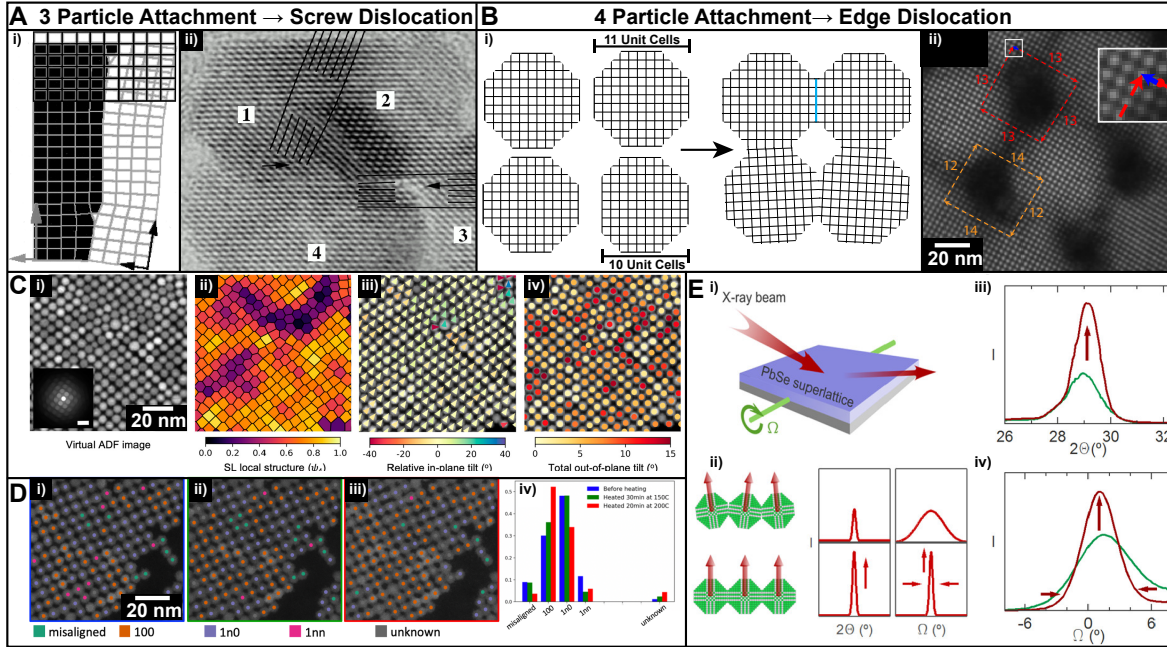
18

Figure 7: Considerations for multiple particle attachment. (A) Formation of a screw dislocation *via* 3 particle attachment. Reproduced with permission from ref 20. Copyright 1998 AAAS. (B i) Attachment of 4 particles with atomically flat facets, but with different sizes leading to a "hollow core" edge dislocation. (B ii) Experimental example of a hollow core edge dislocation resulting from 4 attached PbSe nanocrystals. (B ii) Image reproduced with permission from ref 40. Copyright 2016 American Chemical Society. Burgers circuit annotation added by the current authors. (C) 4D STEM characterization of various order parameters in a PbSe superlattice i) Virtual dark field image, ii) local superlattice structure, iii) in plane tilt of the atomic lattice, and iv) out of plane tilt of the atomic lattice. Reproduced with permission from ref 41. Copyright 2020 American Chemical Society. (D) Improvement of PbSe nanocrystal alignment upon *in situ* thermal annealing. Reproduced with permission from 42. Copyright 2019 Microscopy Society of America. (E) High resolution XRD characterization of PbSe nanocrystal superlattice atomic alignment upon thermal annealing via $2\theta - \Omega$ scans. i) experimental setup, ii) effect of orientational alignment diffraction, iii) experimental 2θ, and iv) Ω scans. Reproduced with permission from ref 43. Copyright 2019 American Chemical Society.

19

open research directions, and the work of Dasilva *et al.* present a powerful characterization framework. Further, the work of Smeaton *et al.* and Walravens *et al.* illustrate that thermal annealing does improve atomic alignment, however even in their samples, annealing does not yet result in uniform atomic alignment within the samples. Refinement of nanocrystal synthesis, or improvement of initial assembly/attachment uniformity may be needed.

6   Conclusion and Perspectives

In this Account we have outlined the framework for considering defects in colloidal inorganic semiconductor nanocrystals. Kinetic factors which are only apparent in nanoscale crystals greatly facilitate defect-free synthesis of nanocrystals. Atomic attachment of nanocrystals leads to many exciting possibilities, however it is also a potent generator of 1D and 2D crystal defects. We demonstrated how dislocation theory and the Burgers vector notation are powerful tools for predicting 1D defect behavior, and provide a predictive guide to identify optimal facets for defect free attachment. We further demonstrated how attachment facet choice can control planar (2D) defect formation, a useful approach to avoiding defects or controllably introducing them into crystals. Finally we highlighted recent progress and challenges understanding attachment and defect generation in multi-particle nanocrystal attachment and atomically fused nanocrystal superlattices.

We take a moment to consider the merits and challenges for attaching nanocrystals into dimer structures and superlattice structures. For a dimer, the nanocrystals can rotate freely, allowing perfect atomic alignment. Superlattices are geometrically frustrated and nanocrystal rotation can be impinged by neighboring nanocrystals, preventing collective alignment. The degree of crystal misalignment $(3° - 15°)$ in attached quantum dot superlattices is much larger than epitaxial growth mechanisms $(<< 1°)$. Ultimately the mistilt between nanocrystals is a source of crystal defects and strain. These challenges indicate it may be possible to achieve pristine materials in dimer structures, however the path is less certain for arrays.

The atomic lattice is the strongest perturbation an electron (or hole) feels, and thus defects in the atomic lattice will strongly affect carriers. Smaller perturbations from mesoscale superlattices may be drown out by atomic scale defects. Future endeavours to understand improvements to nanocrystal assembly and attachment should consider fundamental limits for perfection and importantly whether those limits will be sufficient for engineered miniband structures or other emergent phenomena. We hope the dislocation theory framework for understanding the behavior of defective nanocrystal attachment interfaces outlined here will help identify routes to improve crystal quality in attached nanocrystals. Finally we suggest that nanocrystal attachment may provide a useful synthetic route to desirable planar defects, and thus high defect densities from attachment is a benefit.

Author Information

Notes

The authors declare no competing financial interest

Biographies

Justin Ondry received his B.S.in chemistry/materials science from the University of California, Los Angeles is 2015 where he performed undergraduate research with Prof. Sarah H. Tolbert. He received his PhD in physical chemistry (Advisor: A. Paul Alivisatos) from the University of California Berkeley in 2020. He primarily studied dislocations and their dynamics in imperfectly attached colloidal nanocrystals using *in situ* transmission electron microscopy.

A. Paul Alivisatos is the Samsung Distinguished Professor of Nanoscience and Nanotechnology and a Professor of Chemistry and Materials Science & Engineering at the University of California, Berkeley. Contributions to the fundamental physical chemistry of nanocrystals are the hallmarks of his research group. He was the founding editor of Nano

Letters, a leading scientific publication of the American Chemical Society in nanoscience.

Acknowledgement

Supporting Information Available

The Supporting Information is available free of charge on the ACS Publications website at DOI:XXX

References

1 Ondry, J. C.; Hauwiller, M. R.; Alivisatos, A. P. Dynamics and Removal Pathway of Edge Dislocations in Imperfectly Attached PbTe Nanocrystal Pairs; Towards Design Rules for Oriented Attachment. *ACS Nano* **2018**, *12*, 3178–3189.

2 Ondry, J. C.; Philbin, J. P.; Lostica, M.; Rabani, E.; Alivisatos, A. P. Resilient Pathways to Atomic Attachment of Quantum Dot Dimers and Artificial Solids from Faceted CdSe Quantum Dot Building Blocks. *ACS Nano* **2019**, *13*, 12322–12344.

3 Goldstein, A. N.; Echer, C. M.; Alivisatos, A. P. Melting in semiconductor nanocrystals. *Science* **1992**, *256*, 1425–7.

4 Tolbert, S. H.; Alivisatos, a. P. Size Dependence of a First Order Solid-Solid Phase Transition: The Wurtzite to Rock Salt Transformation in CdSe Nanocrystals. *Science* **1994**, *265*, 373–6.

5 Efros, A. L.; Rosen, M. The Electronic Structure of Semiconductor Nanocrystals. *Annual Review of Materials Science* **2000**, *30*, 475–521.

6 Woodbury, H. H. Diffusion of Cd in CdS. *Phys. Rev.* **1964**, *134*, A492–A498.

7 Anderson, P. M.; Hirth, J. P.; Lothe, J. *Theory of Dislocations Third Edition*; 2017.

8 Queisser, H. J.; Haller, E. E. Defects in Semiconductors: Some Fatal, Some Vital. *Science* **1998**, *281*, 945–950.

9 Takeuchi, S.; Suzuki, K.; Maeda, K.; Iwanaga, H. Stacking-fault energy of II-VI compounds. *Philosophical Magazine A* **1985**, *50*, 171–178.

10 Hanifi, D. A.; Bronstein, N. D.; Koscher, B. A.; Nett, Z.; Swabeck, J. K.; Takano, K.; Schwartzberg, A. M.; Maserati, L.; Vandewal, K.; van de Burgt, Y.; Salleo, A.; Alivisatos, A. P. Redefining near-unity luminescence in quantum dots with photothermal threshold quantum yield. *Science* **2019**, *363*, 1199–1202.

11 Baumgardner, W. J.; Whitham, K.; Hanrath, T. Confined-but-connected quantum solids via controlled ligand displacement. *Nano Letters* **2013**, *13*, 3225–3231.

12 Kalesaki, E.; Delerue, C.; Morais Smith, C.; Beugeling, W.; Allan, G.; Vanmaekelbergh, D. Dirac cones, topological edge states, and nontrivial flat bands in two-dimensional semiconductors with a honeycomb nanogeometry. *Physical Review X* **2014**, *4*, 1–12.

13 Cui, J.; Panfil, Y. E.; Koley, S.; Shamalia, D.; Waiskopf, N.; Remennik, S.; Popov, I.; Oded, M.; Banin, U. Colloidal quantum dot molecules manifesting quantum coupling at room temperature. *Nature Communications* **2019**, *10*, 5401.

14 Boneschanscher, M.; Evers, W. H.; Geuchies, J. J.; Altlantzis, T.; Goris, B.; Rabouw, F.; van Rossum, S. A. P.; van der Zant, H. S. J.; Siebbeles, L. D. A.; Van Tendeloo, G.; Swart, I.; Hilhorst, J.; Petukhov, A.; Bals, S.; Vanmaekelbergh, D. Long-range orientation and atomic attachment of nanocrystals in 2D honeycomb superlattices. *Science* **2014**, *344*, 1377–1380.

15 Whitham, K.; Yang, J.; Savitzky, B. H.; Kourkoutis, L. F.; Wise, F.; Hanrath, T. Charge transport and localization in atomically coherent quantum dot solids. *Nature Materials* **2016**, *15*, 557–563.

16 Shiang, J. J.; Kadavanich, A. V.; Grubbs, R. K.; Alivisatos, A. P. Symmetry of annealed wurtzite CdSe nanocrystals. Assignment to C3vpoint group. *Journal of physical chemistry* **1995**, *99*, 17417–17422.

17 Li, D.; Nielsen, M.; Lee, J.; Frandsen, C.; Banfield, J. F.; De Yoreo, J. J. Direction-Specific Interactions Control Crystal Growth by Oriented Attachment. *Science* **2012**, *336*, 1014–1018.

18 Van Der Stam, W.; Rabouw, F. T.; Vonk, S. J.; Geuchies, J. J.; Ligthart, H.; Petukhov, A. V.; De Mello Donega, C. Oleic Acid-Induced Atomic Alignment of ZnS Polyhedral Nanocrystals. *Nano Letters* **2016**, *16*, 2608–2614.

19 Evers, W. H.; Goris, B.; Bals, S.; Casavola, M.; De Graaf, J.; Roij, R. V.; Dijkstra, M.; Vanmaekelbergh, D. Low-dimensional semiconductor superlattices formed by geometric control over nanocrystal attachment. *Nano Letters* **2013**, *13*, 2317–2323.

20 Penn, R. L.; Banfield, J. Imperfect Oriented Attachment: Dislocation Generation in Defect-Free Nanocrystals. *Science* **1998**, *281*, 969–971.

21 Morrell, M. V.; He, X.; Luo, G.; Thind, A. S.; White, T. A.; Hachtel, A.; Borisevich, A. Y.; Idrobo, J.-c.; Mishra, R.; Xing, Y. Significantly Enhanced Emission Stability

of CsPbBr3 Nanocrystals via Chemically Induced Fusion Growth for Optoelectronic Devices via Chemically Induced Fusion Growth for Optoelectronic Devices. *ACS Applied Nano Materials* **2018**, *1*, 6091–6098.

22 Yuk, J. M.; Park, J.; Ercius, P.; Kim, K.; Hellebusch, D. J.; Crommie, M. F.; Lee, J. Y.; Zettl, A.; Alivisatos, A. P. High-Resolution EM of Colloidal Nanocrystal Growth Using Graphene Liquid Cells. *Science* **2012**, *336*, 61–64.

23 Cai, W.; Nix, W. D. *Imperfections in Crystalline Solids*; 2016.

24 Osipiyan, Y. A.; Smirnova, I. S. Perfect Dislocations in the Wurtzite Lattice. *Physica Status Solidi (b)* **1968**, *30*, 19–29.

25 Osipyan, Y. A.; Smirnova, I. S. Partial dislocations in the wurtzite lattice. *Journal of Physics and Chemistry of Solids* **1971**, *32*, 1521–1530.

26 Jeong, H.-C.; Williams, E. D. Steps on surfaces: experiment and theory. *Surface Science Reports* **1999**, *34*, 171–294.

27 Dalpian, G.; Chelikowsky, J. Self-Purification in Semiconductor Nanocrystals. *Physical Review Letters* **2006**, *96*, 226802.

28 Du, M. H.; Erwin, S. C.; Efros, A. L.; Norris, D. J. Comment on "self-purification in semiconductor nanocrystals". *Physical Review Letters* **2008**, *100*, 179702.

29 Dalpian, G. M.; Chelikowsky, J. R. Dalpian and Chelikowsky reply:. *Physical Review Letters* **2008**, *100*, 179703.

30 Siems, R.; Delavignette, P.; Amelinckx, S. The buckling of a thin plate due to the presence of an edge dislocation. *physica status solidi (b)* **1962**, *2*, 421–438.

31 Thind, A. S.; Luo, G.; Hachtel, J. A.; Morrell, M. V.; Cho, S. B.; Borisevich, A. Y.; Idrobo, J.-C.; Xing, Y.; Mishra, R. Atomic Structure and Electrical Activity of Grain

Boundaries and Ruddlesden-Popper Faults in Cesium Lead Bromide Perovskite. *Advanced Materials* **2018**, *1805047*, 1805047.

32 Sarkar, S.; Acharya, S.; Chakraborty, A.; Pradhan, N. Zinc blende 0D quantum dots to wurtzite 1D quantum wires: The oriented attachment and phase change in ZnSe nanostructures. *Journal of Physical Chemistry Letters* **2013**, *4*, 3292–3297.

33 Huang, F.; Zhang, H.; Banfield, J. F. Two-stage crystal-growth kinetics observed during hydrothermal coarsening of nanocrystalline ZnS. *Nano Letters* **2003**, *3*, 373–378.

34 Tsai, M. H.; Chen, S. Y.; Shen, P. Imperfect oriented attachment: Accretion and defect generation of nanosize rutile condensates. *Nano Letters* **2004**, *4*, 1197–1201.

35 Yuan, Y.; Wood, S. M.; He, K.; Yao, W.; Tompsett, D.; Lu, J.; Nie, A.; Islam, M. S.; Shahbazian-Yassar, R. Atomistic insights into the oriented attachment of tunnel-based oxide nanostructures. *ACS Nano* **2016**, *10*, 539–548.

36 Vermaut, P.; Nouet, G.; Ruterana, P. Observation of two atomic configurations for the 1120 stacking fault in wurtzite (Ga, Al) nitrides. *Applied Physics Letters* **1999**, *74*, 694–696.

37 Dick, K. A.; Thelander, C.; Samuelson, L.; Caroff, P. Crystal phase engineering in single InAs nanowires. *Nano Letters* **2010**, *10*, 3494–3499.

38 Ruddlesden, S. N.; Popper, P. The compound Sr 3 Ti 2 O 7 and its structure . *Acta Crystallographica* **1958**, *11*, 54–55.

39 Qian, W.; Rohrer, G. S.; Skowronski, M.; Doverspike, K.; Rowland, L. B.; Gaskill, D. K. Open-core screw dislocations in GaN epilayers observed by scanning force microscopy and high-resolution transmission electron microscopy. *Applied Physics Letters* **1995**, *67*, 2284.

40 Savitzky, B. H.; Hovden, R.; Whitham, K.; Yang, J.; Wise, F.; Hanrath, T.; Kourk-outis, L. F. Propagation of Structural Disorder in Epitaxially Connected Quantum Dot Solids from Atomic to Micron Scale. *Nano Letters* **2016**, *16*, 5714–5718.

41 Dasilva, J. C.; Smeaton, M. A.; Dunbar, T. A.; Xu, Y.; Balazs, D. M.; Kourkoutis, L. F.; Hanrath, T. Mechanistic Insights into Superlattice Transformation at a Single Nanocrys-tal Level Using Nanobeam Electron Diffraction. *Nano Letters* **2020**, *20*, 5267–5274.

42 Smeaton, M. A.; Balazs, D. M.; Hanrath, T.; Kourkoutis, L. F. Quantifying Atomic-Scale Quantum Dot Superlattice Behavior Upon *in situ* Heating. *Microscopy and Microanalysis* **2019**, *25*, 1538–1539.

43 Walravens, W.; Solano, E.; Geenen, F.; Dendooven, J.; Gorobtsov, O.; Tadjine, A.; Mah-moud, N.; Ding, P. P.; Ruff, J. P.; Singer, A.; Roelkens, G.; Delerue, C.; Detavernier, C.; Hens, Z. Setting Carriers Free: Healing Faulty Interfaces Promotes Delocalization and Transport in Nanocrystal Solids. *ACS Nano* **2019**, *13*, 12774–12786.

44 Kopp, V. S.; Kaganer, V. M.; Baidakova, M. V.; Lundin, W. V.; Nikolaev, A. E.; Verkhovtceva, E. V.; Yagovkina, M. A.; Cherkashin, N. X-ray determination of thread-ing dislocation densities in GaN/Al2O3(0001) films grown by metalorganic vapor phase epitaxy. *Journal of Applied Physics* **2014**, *115*.

Graphical TOC Entry

Imperfect Nanocrystal Attachment → Defective Interface → i) ii) iii) Bulk Crystal Dislocation Theory → Perfect Interface